Iraqi Journal of Science

ISSN: 0067-2904
GIF: 0.851

Preparation and Characterization of Yttrium Oxide Nanoparticles at Different Calcination Temperatures from Yttrium Hydroxide Prepared by Hydrothermal and Hydrothermal microwave Methods

Ahlam J. Abdulghani * and Waleed M. Al- Ogedy
Department of Chemistry, College of Science, University of Baghdad, Baghdad, Iraq

Abstract

The Synthesis of yttrium oxide nanoparticles have been achieved via calcination of yttrium hydroxide produced from the reaction of aqueous solutions of yttrium nitrate and sodium hydroxide at pH = 13 using hydrothermal and hydrothermal microwave methods. Effect of heat treatment of the resulted yttrium hydroxide powder on the morphology and crystallinity of the resulting oxide was studied at calcination 500, 700 and 1000°C to obtain. The resulted products were characterized by means of X-ray diffraction (XRD), scanning electron microscope (SEM), atomic force microscope (AFM), Fourier transform infrared spectrometer (FTIR) and thermal analyses (TG).

Keywords: hydrothermal method, nanorods, Scherre's equation

تحضيروتشخيص دقائق اوكسيد الاتريوم النانوية في درجات حرارة تلدين مختلفه من هيدروكسيد الاتريوم المحضر بطريقتي الهيدروحرارية والهيدروحراريه ـ الموجات الدقيقة

احلام جميل عبد الغني* و وليد مظلوم العكيدي
قسم الكيمياء، كلية العلوم، جامعة بغداد، بغداد، العراق

الخلاصة

تم تحضير دقائق اوكسيد الاتريوم النانوية من تسخين هيدروكسيد الاتريوم المحضر من نترات الاتريوم مع هيدروكسيد الصوديوم في الدالة الحامضية 13 باستخدام طريقتي الهيدروحراري الاعتيادي والهيدروحراري باستخدام اشعة الموجات الدقيقة .تمت دراسة تاثير المعاملة الحرارية للهيدروكسيد الناتج على الهيئة البلورية واشكال مسحوق الاوكسيد النانوي الناتج في درجات التلدين 500و700و1000° م. شخصت النواتج باعتماد تحاليل حيود الاشعة السينية والمجهر الالكتروني الماسح ومجهر القوة الذرية ومطيافية الاشعة تحت الحمراء والتحاليل الحرارية

Introduction:

Yttrium oxide or yttria is one of the most stable yttrium compounds with a very wide range of important applications. The synthesis methods play an important role to produce the required size and morphology of nanoparticles as main controlling factors for each application. Several methods have been suggested for the preparation of yttrium oxide nanoparticles such as chemical precipitation [1-5], sol gel [6-8], electro thermal decomposition [9], solvothermal [10], hydrothermal [10-13], combustion synthesis [14-17], sonochemical methods [18], reverse micelle method [19], microwave hydrothermal [20], microwave solvothermal [21] and microwave combustion methods [22-24]. In terms of energy saving , safety, and controlled high yield synthesis of highly crystallized products, the hydrothermal and microwave hydrothermal methods are being more favored compared with the others [,20 25,26]. The reaction pH, metal precursors, reactant concentrations, reaction time and annealing or calcination temperatures are the main controlling factors of sizes and morphology of these nanoparticles [1,9,10,11,13,26-28]. The type of precipitating base as well as addition time may also give rise to different morphology of Y_2O_3 nanostructures [13, 25]. In this work we report the synthesis of two different morphologies of Y_2O_3 : nano rod and worm- neck-structured nanoparticles from

*Email: ahlamjameel@scbaghdad.edu.iq

calcination of yttrium hydroxide synthesized via hydrothermal and microwave hydrothermal reaction processes respectively, using $Y(NO_3)_3$ as a precursor salt and 0.3M NaOH as a precipitant. In this comparison between the two methods, we study the effect of calcination temperature at 500°C, 700°C and 1000°C on size and morphology of the resulting oxide. The resulted products were characterized by means of X-ray diffraction (XRD), scanning electron microscope (SEM), atomic force microscope (AFM), Fourier transform infrared spectrometer (FTIR) and thermogravimetric a analyses (TGA).

Experimental

Materials

High-purity 99.9% Y $(NO_3)_3.6H_2O$, was purchased from Sigma Aldrich. Sodium hydroxide NaOH 96% was used as received from BDH. Aqueous solutions of metal precursor and sodium hydroxide were prepared using doubly distilled deionized water (DDW)

Instruments

Purification of the prepared $Y(OH)_3$ from unreacted species and by products was achieved by centrifugation of colloids using Centrifuge instrument (6000 rpm) type Jouan C_4 S.A.S France . FT-IR spectra for the powders were recorded at room temperature with FT-IR spectrophotometer type SHIMADZU 8400 S FT-IR using KBr pellet. SEM Scanning electron microscope images were acquired using type TE SCAN VEGA 2 Cheech. A few products put on grid and disperse to Characterization. AFM Atomic force microscope images were acquired using AFM model AA 3000 SPM 220V Angstrom Advanced INC.USA. samples were prepared by applying few drops of nanoparticles dispersed in acetone, by sonication for 20 min, on a glass slide followed dried to Characterization**.** Thermal gravimetric analyses (TGA) were performed using Perkin Elmer TGA 4000**.** (XRD) patterns were recorded with SHIMADZU 6000 X-Ray Diffract meter with a high-intensity Cu K α radiation (λ=1.54180Å) and a graphite monochromatic source. The as-prepared purified samples of $Y(OH)_3$ and Y_2O_3 nanopowders were sonicated to achieve complete dispersion in DDW, and then applied on a glass slide followed by air drying on a spin coater upon deposition onto glass slides.

Synthesis of Y_2O_3 by hydrothermal method

To a solution of $Y(NO_3)_3.6H_2O$ (4.5 mmol , 1.723gm) dissolved in 12 mL of DDW was added drop wise of an aqueous solution of NaOH (O.3 M, 44 mL) . The addition process took (30) minutes with continuous stirring until the final pH of the reaction mixture was adjusted to 13 by which a white colloid of $Y(OH)_3$ was formed. Then the mixture was left under vigorous stirring for 1 h, to ensure a homogeneous dispersion. The mixture was transferred into a 72 mL homemade Teflon-lined stainless steel autoclave which was subsequently sealed with a stainless steel cover fitted with a stainless steel temperature probe containing a thermocouple inserted in a heating coil connected to a temperature regulator board Figure-1. Temperature was adjusted and maintained at (~200 °C) for 2h, and then gradually regulated to (180 °C) for 5h. The cell was left to cool to room temperature naturally. The colloidal mixture of $Y(OH)_3$ was centrifuged at 6000 rpm for 15 min and the precipitate was washed several times with deionized water until the pH of supernatant solution reached 7. The precipitate was then dried at 80 °C in air for 10h. Finally, the product was divided into four parts , one part for XRD analysis compared with XRD pattern of the compound (space group: JCPDS Nos. 24-1422), and three parts were placed into three ceramic crucibles for annealing at 500, 700 and 1000 °C for 3 h in a box furnace to be converted into the corresponding of Y_2O_3 nanopowder

Synthesis Y_2O_3 by microwave hydrothermal method

To a solution of Y $(NO_3)_3.6H_2O$ (3.0 mmol , 1.149 gm) dissolved in 8 ml of DDW was added drop wise an aqueous solution of NaOH (O.3 M, 16ml) within a period of (30) minutes with continuous stirring until the final pH of the reaction mixture was adjusted to 13and the mixture was further stirred for 1 h,. The milky colloid solution was transferred into a 30 mL homemade teflon autoclave (Figure -2) which was subsequently sealed and placed into a domestic microwave oven (LG, MS2042X frequency 2.450 MHz, maximum power 1000 W, multimode oven) starting operating at third level for 15 minuet ((9) second ON and(14) second OFF) which was kept at temperature range 240-250°C. The oven was fitted with a wireless camera to watch capsule reactor.

Figure 1- a-Hydrothermal reaction autoclave, b- An electric temperature regulating control board

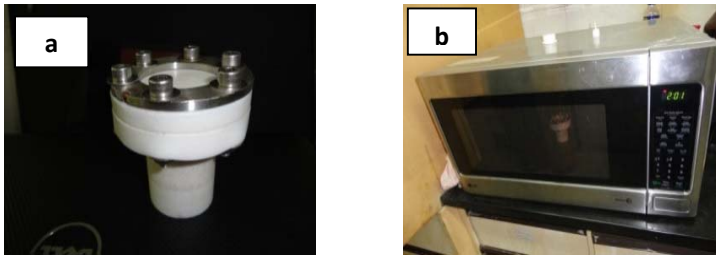

Figure 2- a-Microwave cell, b-Microwave instrument

The cell was left to cool to room temperature naturally and the colloid was then centrifuged for 15 min. The precipitate was washed from impurities with deionized water several times until the pH of supernatant solution reached 7. The product was then treated similarly as previously mentioned in the hydrothermal process.

Result and Discussion

XRD analysis

Powder X-ray diffraction (XRD) patterns of $Y(OH)_3$ prepared by hydrothermal and microwave heat treatment processes are shown in Figures (3a and b respectively). The main peaks observed in Figure (3a) at 2θ 16.46°, 28.5°, 30.2°, 38°, 42.2°, 50.1°, 51.4° correspond respectively, to the planes(100),(110),(101), (111), (201), (300), (211) [14, 29] and are in agreement with the structures of hexagonal $Y(OH)_3$ (space group: JCPDS Nos. 24-1422) with lattice parameters a=b= 6.268 A° and c=3.546 A° for X-ray diffract meter with a high-intensity Cu K α radiation. The spectrum of microwave synthesized yttrium hydroxide (Figure -3-b) exhibited peaks at 2θ 28.5°,30.2°, 38°, 42.2°,50.1° corresponding to the planes (110), (101),(111), (201),(300) respectively which also indicated that the product could be indexed to a pure hexagonal phase of $Y(OH)_3$ [14, 29] (space group: JCPDS Nos. 24-1422). The peaks around 11.2°,19.5° and 21.5,° in figure-3-a and the broad peak at 2Θ =21.5° in figure 3b refer to yttrium hydroxyl nitrate [26,30] and were in agreement with JCPDS Nos.79-1352.

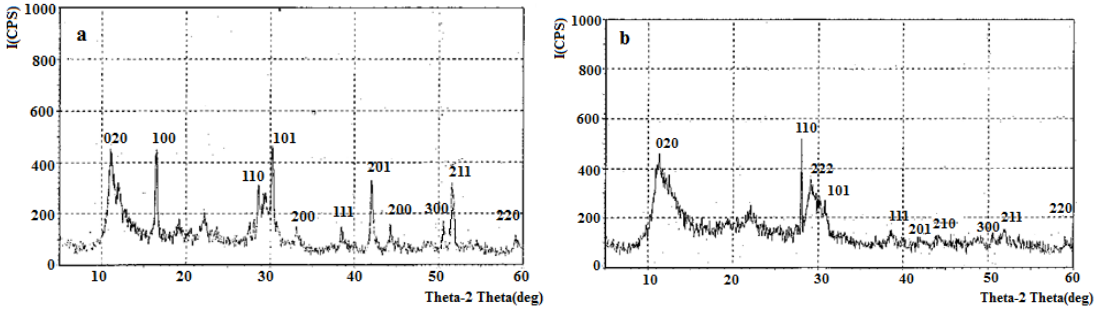

Figure 3- XRD patterns for yttrium hydroxide synthesized by a- by hydrothermal and, b-by microwave methods

Various results have been obtained in the literature concerning the effect of calcination temperature and annealing time on the transformation of yttrium hydroxide nanostructures and on the crystal structure, morphology and sizes of the resulting products [14, 29]. In this work calcination was adopted at three different temperatures: 500° C, 700°C and 1000° C. Figures -4and -5 -(a, b, c) show

the XRD diffraction peaks obtained for yttrium hydroxide samples annealed at 500°C, 700°C and 1000°C. The main peaks were observed at 2θ = 20.6°, 29.3°, 33.9°, 48.5°, and 57.6°, corresponding, respectively, to the planes (211),(222), (400), (440),and (622) which confirms the formation of single-phase cubic crystalline yttrium nanoparticles. These patterns are in agreement with the known cubic structures (space group: JCPDS card Nos 25-1200 X-ray diffract meter with a high-intensity Cu K α radiation (α=1.54056Å) and a graphite monochromatic) [6, 31-36]. The estimated average crystallite sizes (L) of Y_2O_3 nanoparticles was calculated from Scherer's formula [36]:

$$L = \frac{K.\ \lambda}{\beta \cos \theta}$$

Where λ is the X-ray wavelength in nanometer (nm), β is the peak width of the diffraction peak profile at half maximum height resulting from small crystallite size in radians and K is a constant related to crystallite shape, normally taken as 0.9 and Theta θ is the diffraction angle. In addition to the Y_2O_3 peaks, one peak was observed at 2θ 11.2° in the XRD patterns of nanocrystalline samples obtained at annealing temperature 500° C and to less extent at 700°C, (Figures 4,5 a and b)) corresponding to the plane (020) of yttrium hydroxynitrate which refers to incomplete transformation

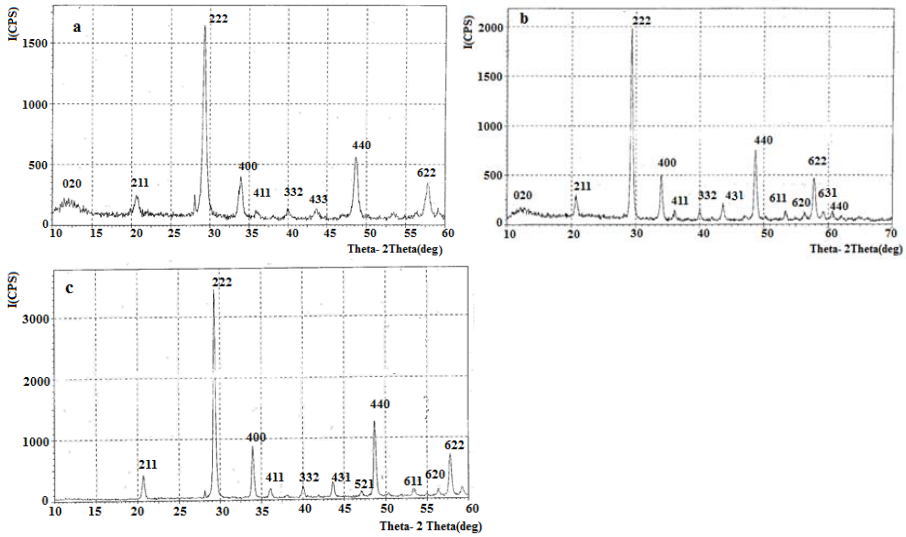

Figure 4- XRD patterns of Y_2O_3 obtained from hydrothermally synthesized yttrium hydroxide precursor at calcination temperatures: (a) 500°C (b) 700°C and (c) 1000°C

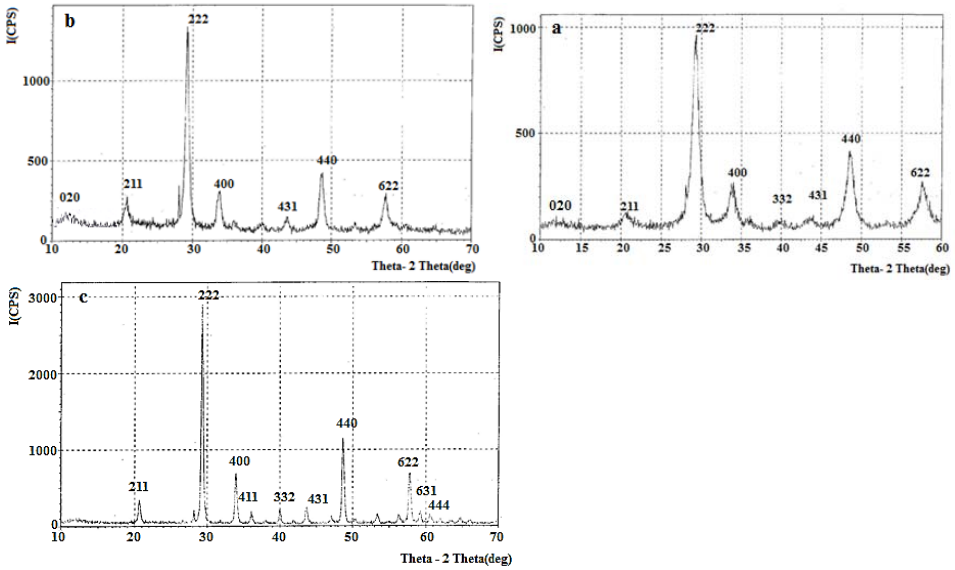

Figure 5 - XRD patterns of the Y_2O_3 obtained from calcination of yttrium hydroxide precursor synthesized by microwave method at (a) 500° (b) 700 and (c) 1000° C

Of some of the hydroxides to Y_2O_3 [14,37, 38]. Tables 1 and 2 describe the calculated particle size ranges obtained from the data recorded for the main peaks of XRD pattern of Y_2O_3 produced after calcination of hydrothermal and microwave hydrothermally synthesized yttrium hydroxide At 1000°C, the XRD patterns in Figures (4c) and (5c) were fully assigned to crystalline Y_2O_3 nano particles which indicates yttrium hydroxide $Y(OH)_3$ was transformed completely into Y_2O_3 nanocrystals [1, 39,40]. The observed peaks corresponded respectively to the (222), (400), (411), (332), (431), (440), (611), and (622) of single-phase cubic crystalline yttrium nanoparticles came in agreement with the JCPDS 41-1105 reference. Depending on the data recorded from main peaks at 2θ 29.32, 33.93, and 48.66 °, the calculated average crystallite sizes of Y_2O_3 nanoparticles obtained from hydrothermally synthesized yttrium hydroxide precursor at annealing temperatures 500, 700 and 1000°C were: 17.13, 24.1and 30.3 nm respectively, while the average crystallite sizes of Y_2O_3 nanoparticles obtained from microwave synthesized yttrium hydroxide precursor were: 8.1, 13.2 and 28.6 nm respectively. The intensity of the diffraction peaks were found to increase with annealing temperatures which refers to improved crystallinity of Y_2O_3. The widths of the diffraction peaks also decreased due to the increasing particle size.

Table 1- Average particle size of Y_2O_3 obtained from calcination of hydrothermally synthesized yttrium hydroxide at different temperatures using Sherrer's equation.

Peak at 2Θ (deg)	d(A°)	FWHM	Sizediameter(nm)	Average size diameter (nm)	Morphology (SEM)
500°C					
29.32°	3.043	0.501	21.5	17.13	Rods
33.93°	2.639	0.572	14.09		
48.66°	1.860	0.553	16.0		
700°C					
29.35°	3.039	0.408	29.03		
33.98°	2.635	0.382	20.5	24.1	Rods
48.70°	1.868	0.427	23.0		
1000°C					
29.34°	3.043	0.298	30.0	30.3	
33.47°	2.636	0.299	32.8		Rods+few irregular shaped nanocrystals
48.68°	1.868	0.271	28.1		

Table 2- Average particle size of Y_2O_3 obtained from calcination of yttrium hydroxide synthesized by microwave hydrothermal method using Sherrer's equation

Peak at 2Θ	d(A°)	FWHM	Size diameter (nm)	Average size diameter (nm)	morphology
500°C					
29.29°	3.046	0.969	8,6	8.1	Wires
48.57°	1.872	1.010	8.1		
57.67°	1.596	1.132	7.8		
700°C					
29.23°	3.052	0.641	13.8	13.2	Wires
33.859°	2.64	0.715	13.5		
48.59°	1.871	0.711	12.6		
1000°C					
29.33	3.042	0.3054	32.5	28.6	Worm-neck structure100%
48.69°	1.872	0.3059	27.0		
57.77°	1.594	0.330	26.0		

FTIR Spectra

The FTIR spectrum of yttrium hydroxide precursors obtained from hydrothermal and microwave processes are shown in Figures – 6-a and(- 7-a) respectively while those obtained after annealing the prepared hydroxides at 1000 °C are shown in Figures – 6-b and(- 7-b) respectively . The peaks observed in the region 3647.14 -3403.46 cm^{-1} and at 1508.23 cm^{-1} can be assigned to OH stretching and bending vibration modes, respectively resulting from both hydroxyl groups and strongly adsorbed

molecular water in the crystal lattice of yttrium hydroxide [1,41]. The peaks around 1640 and 1555 cm^{-1} are assigned to asymmetric stretching of C–O band which may arise from the absorption of CO_2 from the atmosphere. It is well known that, yttrium hydroxide, like other lanthanides, can absorb CO_2 from the atmosphere during precursor drying and/or exposure of dried powder to the air [42]. The peaks at about 1540 and 1406 cm^{-1} can be attributed to the split symmetric antisymmetrical stretching vibration of carbonate and nitrate group, respectively [9, 39].The peaks observed at 1384.7 cm^{-1} may be assigned to vibrational modes of nitrate ion of some unconverted hydroynitrate intermediate [9, 11]. The peaks between 549.67 – 738.69 cm^{-1} are attributed to the Y–O stretching vibration resulting from hydroxide and nitrate bonds with yttrium ion [9] . After the precursor was calcined at 1000°C for 3h (Figure -6-b), the spectrum exhibited the disappearance of the bands assigned vibrational modes of lattice water and decreased intensity of the peaks assigned to stretching modes of carbonate and nitrate vibrations. New bands appeared at 565.1, and 497 cm^{-1} were assigned to the stretching vibration of Y–O of Y_2O_3 molecules [9,30,31].

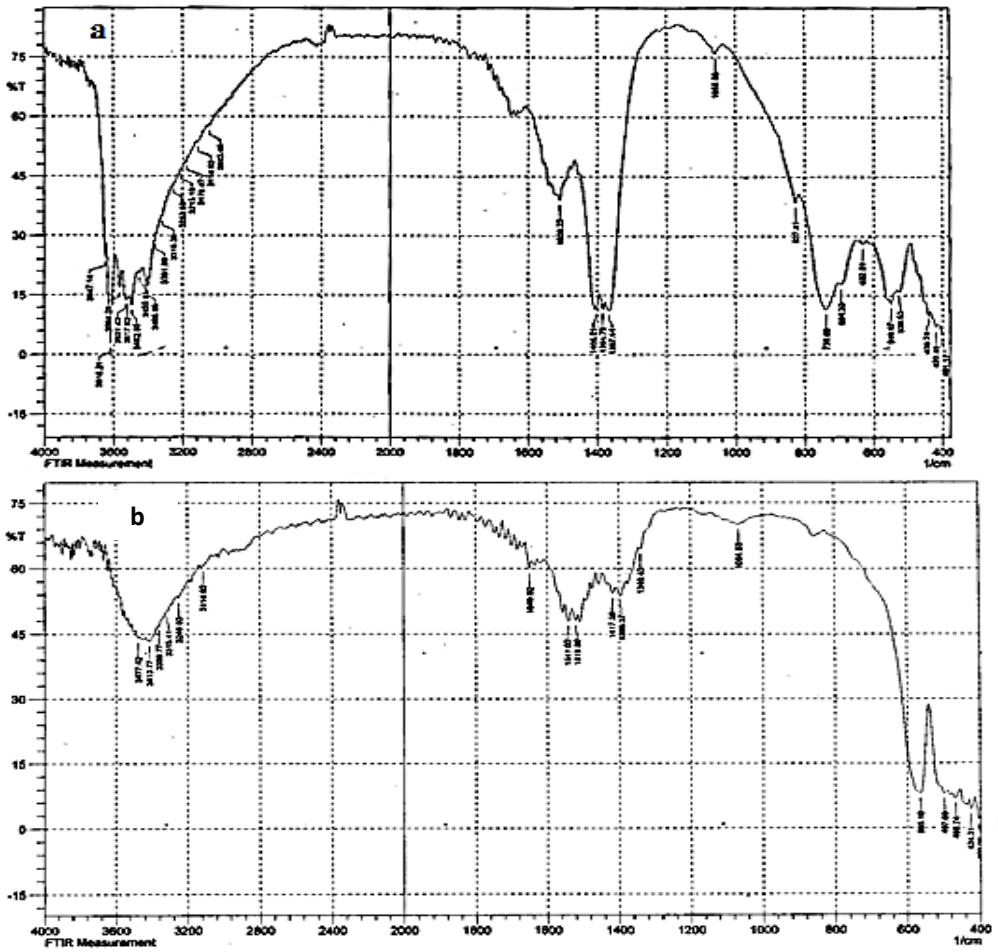

Figure 6- The FTIR spectra of a-$Y(OH)_3$ produced by hydrothermal method and b- Y_2O_3 nanoparticles at calcination temperature 1000 °C

The FTIR spectrum of yttrium hydroxide precursor synthesized by microwave process (Figure -7-a) exhibited the peaks assigned to the presence of water molecules in the crystal lattice which was demonstrated by the appearance of OH stretching and bending vibrations in the region 3645.21- 3200 and at 1508.23 cm^{-1} respectively [1,41,43]. The peaks observed at 1530- 1519.8 and 1409.87-1384.79 are attributed to carbonate and nitrate group vibrations respectively [9, 35]. The bands observed at 526.53-694.33 cm-1 are assigned to the stretching vibration of Y–O bonds [42]. After annealing the prepared hydroxide at 1000 °C, the FTIR spectrum of the resulting Y_2O_3 (Figure -7-b) exhibited the disappearance of the bands related to lattice water molecules and nitrate groups and highly decreased

intensity of the bands assigned to the carbonate group. The new band appeared at 567 cm^{-1} assigned to Y-O stretching vibrations [9,30]. The peaks observed in the frequency region 3470 -3200 cm^{-1} for both oxides may be assigned to vibrational mode of OH resulting from the presence of moisture in KBr disc.

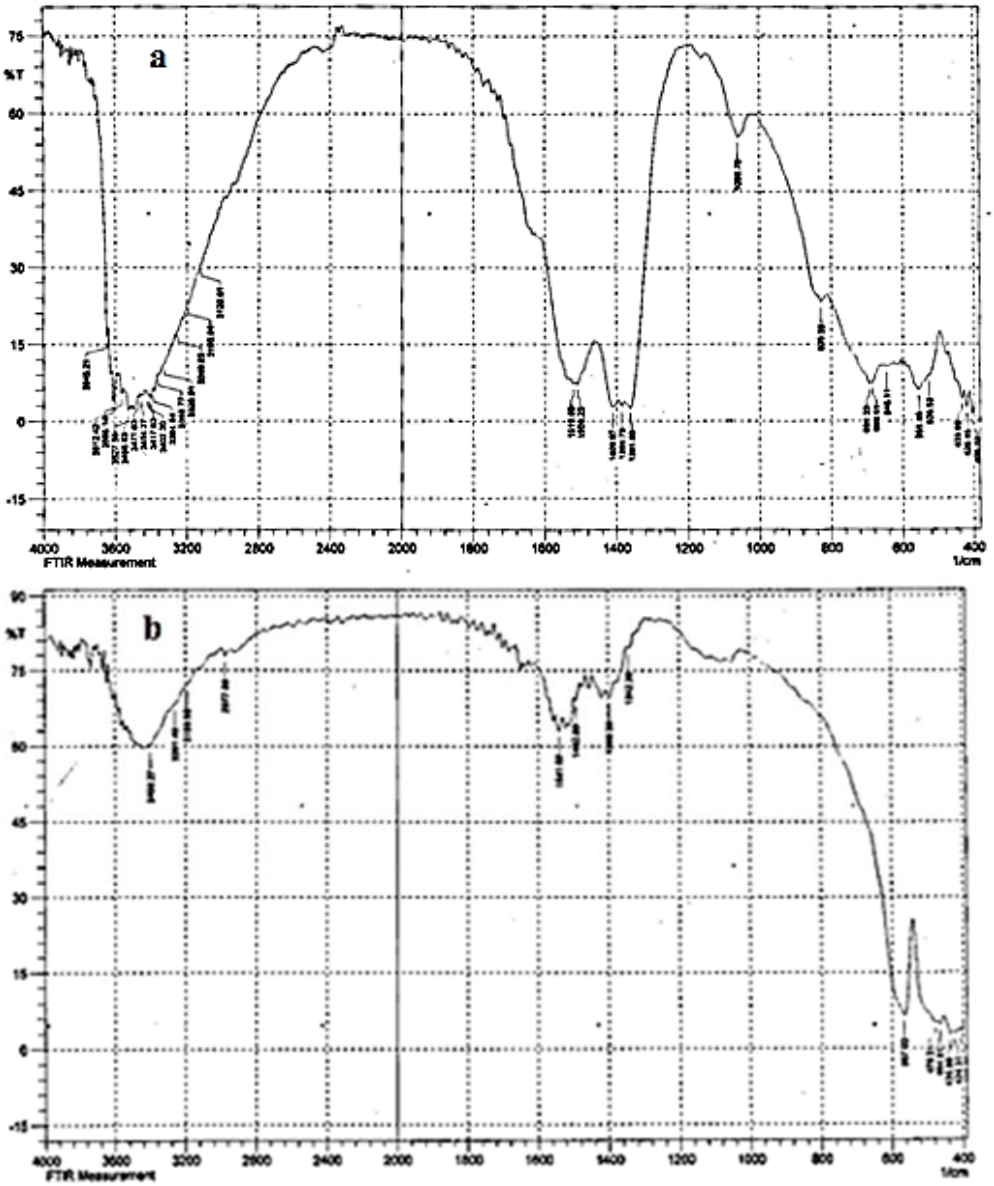

Figure 7-The FTIR spectra of a -yttrium hydroxide precursor produced by microwave method and b- Y_2O_3 nanoparticles obtained at calcination temperature 1000 °C

Scanning Electron microscope

The SEM micrographs show that the morphology of the Y_2O_3 nanoparticles obtained in both methods varied with calcination temperature. Calcination of hydrothermally synthesized yttrium hydroxide at 500, 700 and 1000 °C (Figures -8-a-c respectively) gave rise to nano rods with average diameter of 18.4, 25.4 and 31.1 nm respectively (Figures (8d-f) respectively) and length of (86-240) nm. Calcination of microwave synthesized hydroxide at 500°C and 700°C gave nanowire shaped structures with diameter ranges of (4-20) and (7.2-25) nm respectively and wire length range (31-186) and (35-182) nm respectively (Figures -9-a and -b). At calcination temperature 1000 °C, uniform

nanostructures with worm- neck like shapes were obtained with size diameter range (11.6-36.8) nm (Figure -9-c). The particle size distributions are shown in Figures -9d- f respectively.

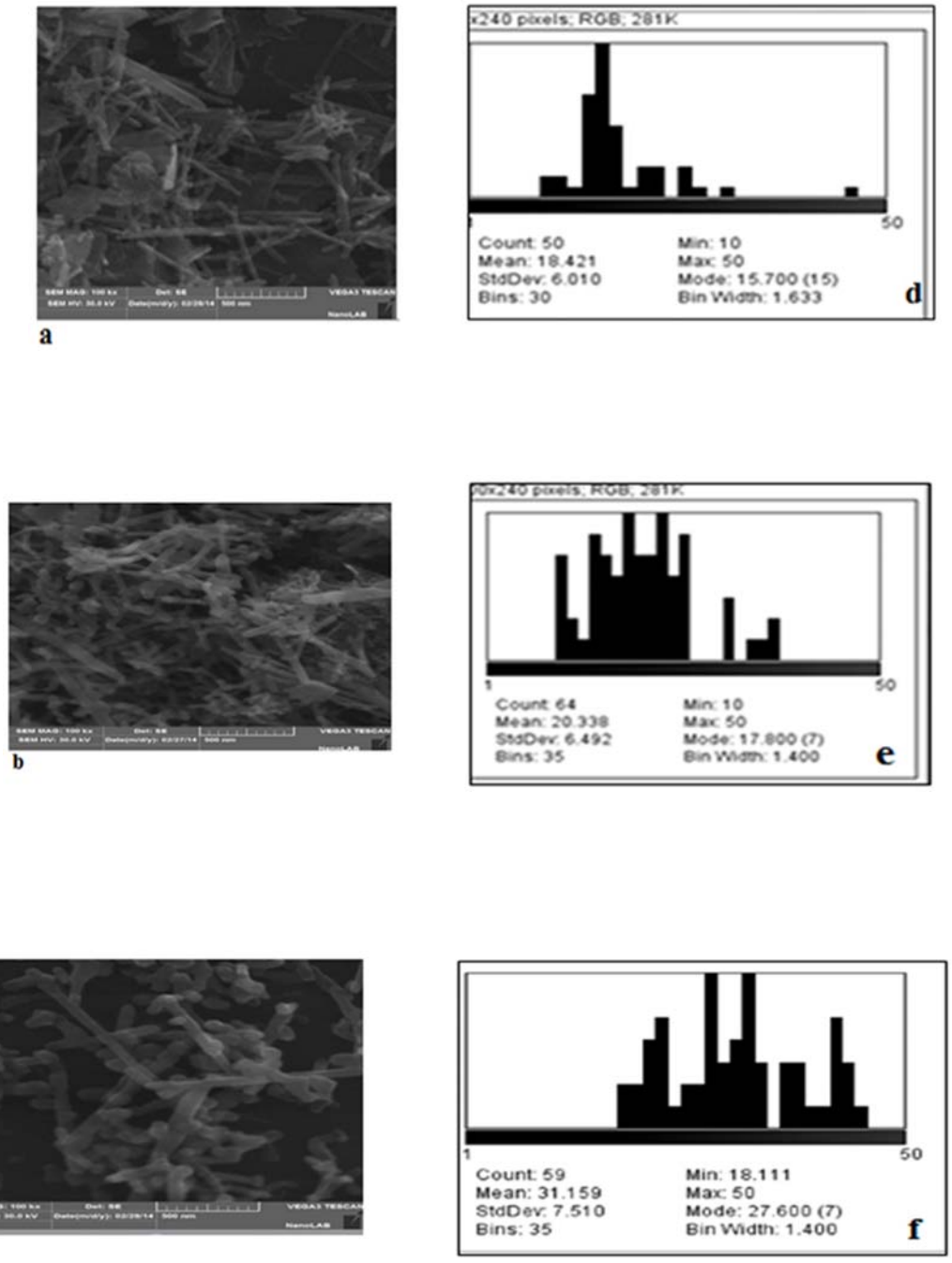

Figure 8- SEM micrographs of Y_2O_3 nanorods obtained from hydrothermally synthesized yttrium hydroxide on calcination at .a- 500°C (b) 700°C (c) 1000°C and diameter size distribution of the three nanostructures (d, e, f respectively)

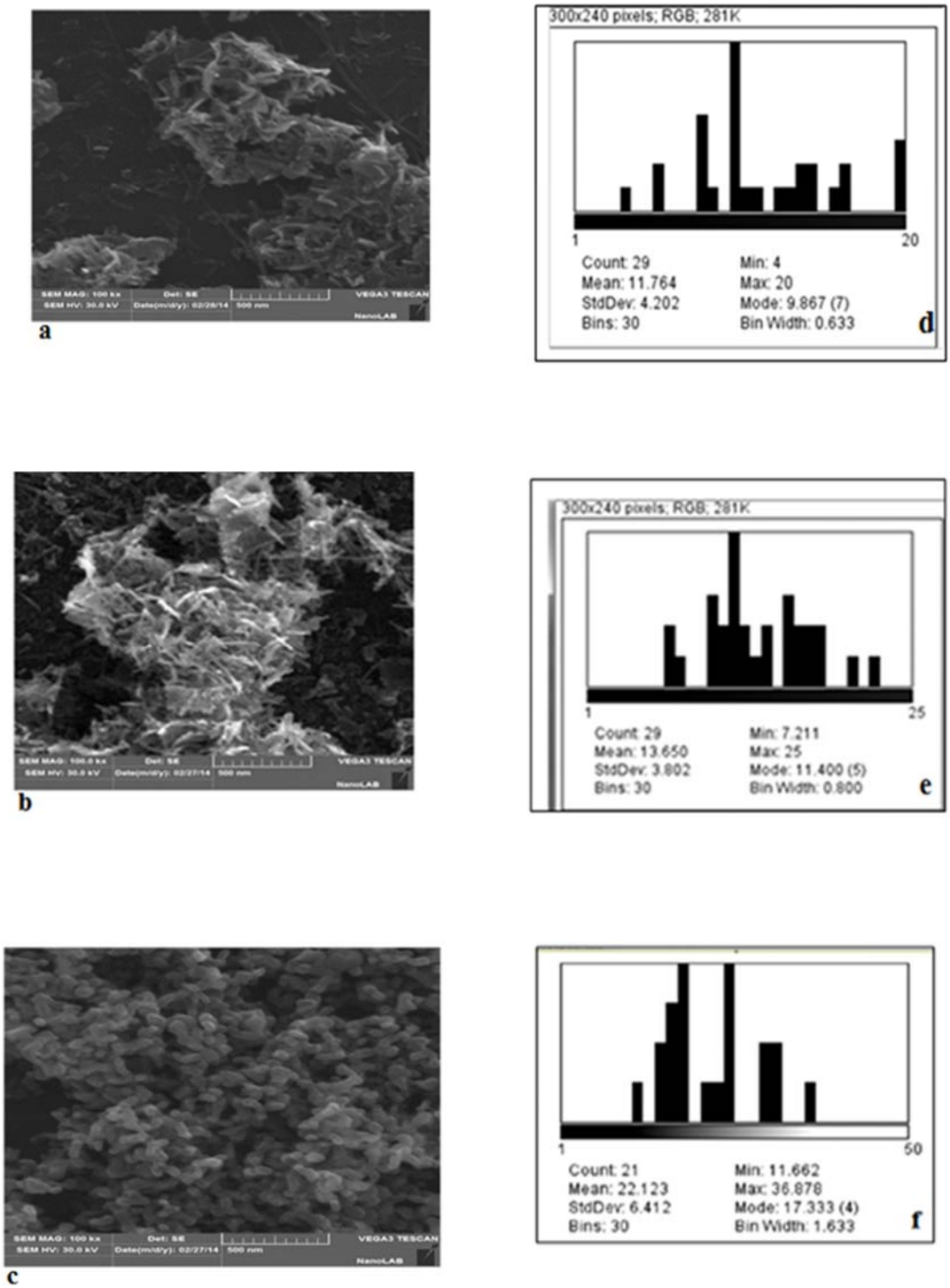

Figure 9- SEM micrographs of Y_2O_3 nanostructures obtained from calcination of microwave hydrothermally synthesized yttrium hydroxide at 500°C 700°C and 1000° C (-a,-b and -c respectively) with diameter size distribution of the three nanostructures (-d, -e, -f respectively)

Atomic Force Microscope

Figures -10 and -11 show the AFM images of yttrium oxide nanoparticles obtained respectively from calcination of hydrothermal and microwave hydrothermally synthesized yttrium hydroxide at 1000°C. The morphologies of these nanoparticles agreed with those obtained from the SEM micrographs at the same temperature. The average sizes of nanoparticles were about 52.5 and 66.73nm respectively.

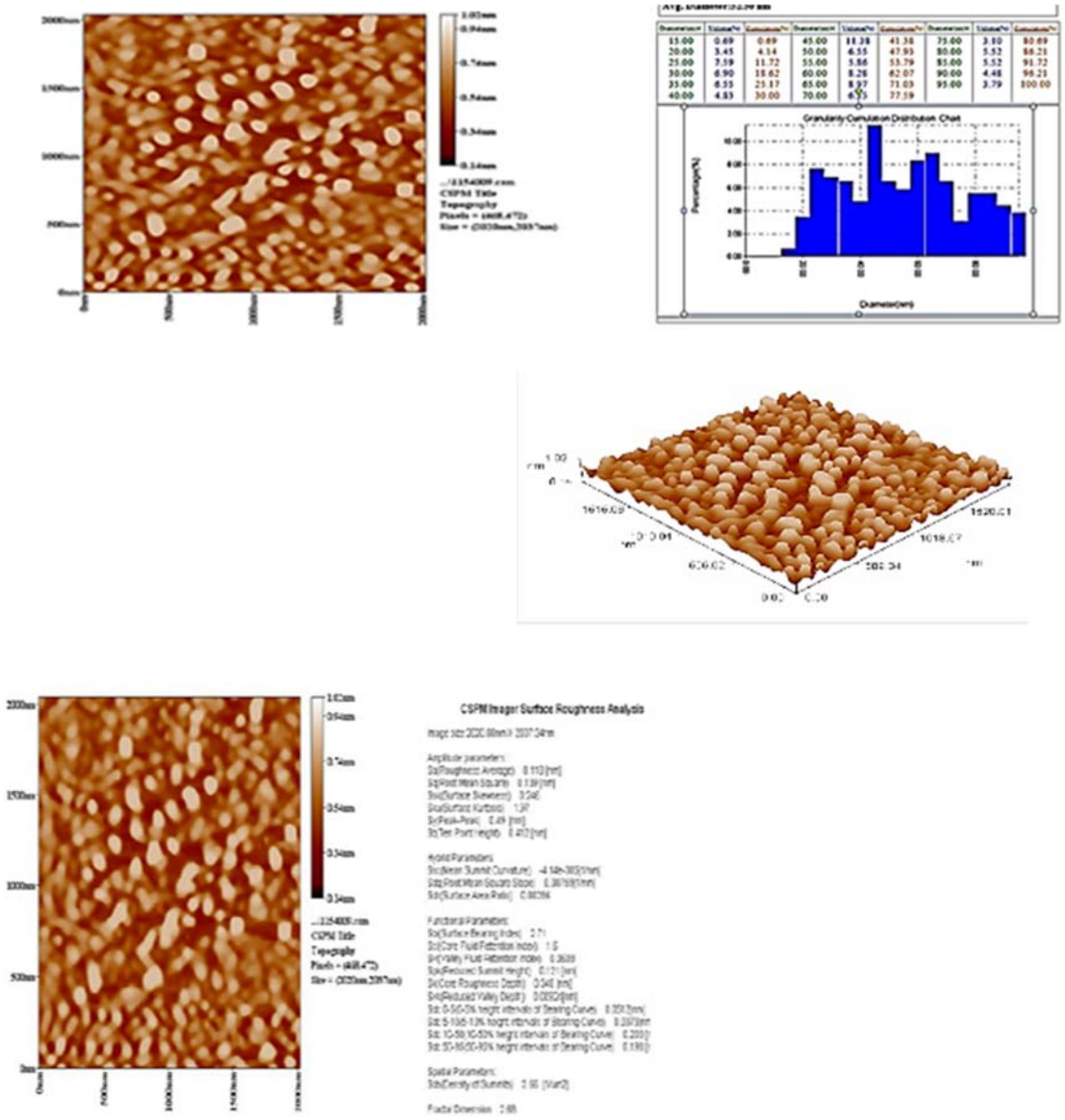

Figure 10- AFM 2D and 3D views and particle size distribution of Y_2O_3 by obtained calcination of hydrothermally synthesized yttrium hydroxide at 1000°C

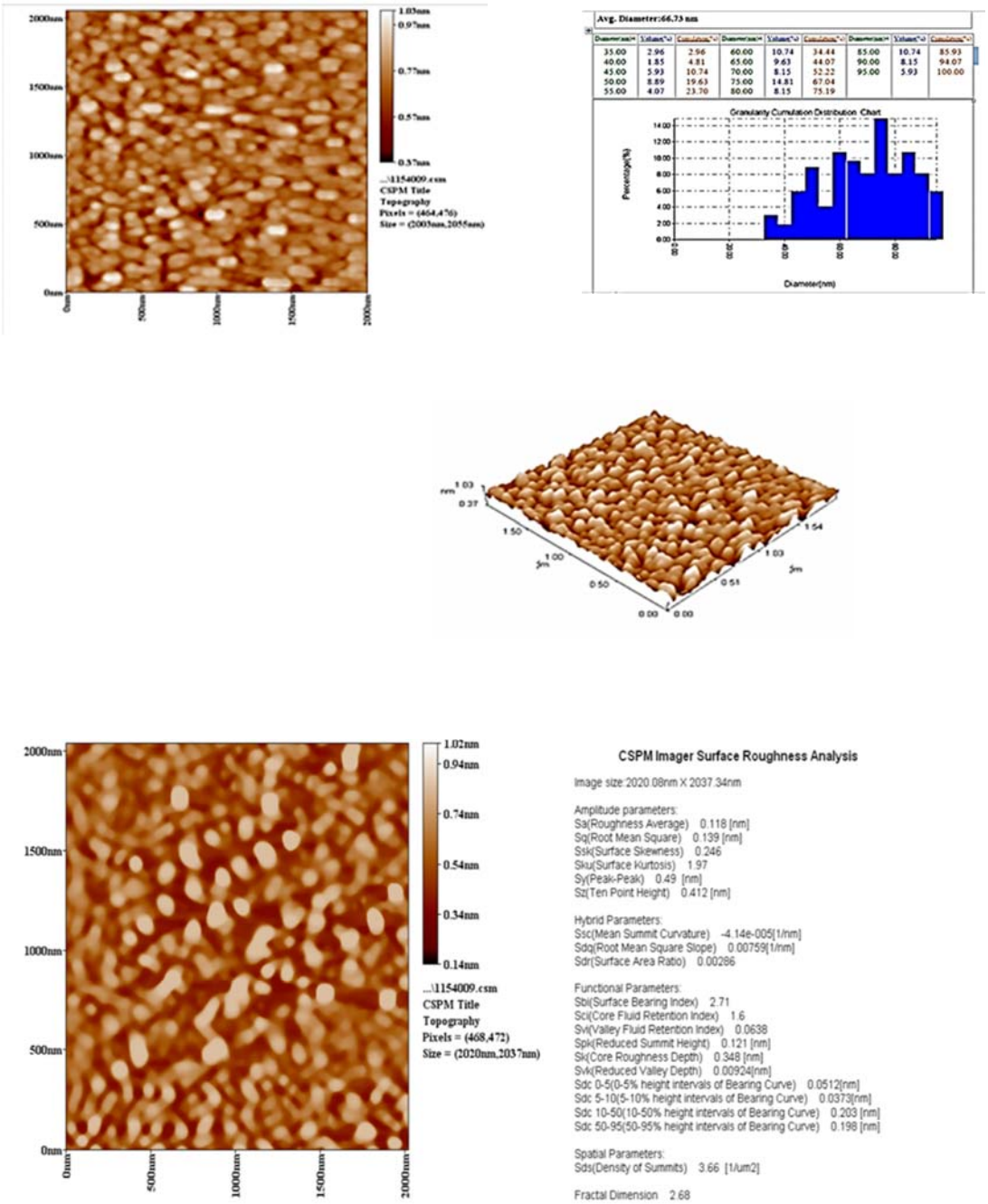

Figure 11- AFM 2D and 3D views and particle size distribution of Y_2O_3 obtained by calcination of microwave synthesized yttrium hydroxide at 1000° C

Thermal gravimetric analysis

The TG curve of the as-prepared yttrium hydroxide precursor by hydrothermal method shown in Figure (-12 -a) shows that the compound was stable up to 236 °C. Then the curve displayed two steps of thermal decomposition with a total weight loss of about 18.43%. In the first step, a weight loss of 12.1% occurred at temperature range 236-336°C at peak temperature 273.2 °C as was indicated by the DTG curve. This step was attributed to the loss of about 2.2 H_2O molecules which leads to the partial conversion of the hydroxide precursor to yttrium oxide [11]. In the second step, a weight loss of 6.33% took place at temperature range 336-400 °C at peak temperature 366.2 °C. This step was attributed to the removal of the loss of remaining water ($0.7H_2O$, 3.95%) and the thermal decomposition of the existing nitrate ($0.2NO_2$, 2.88%).

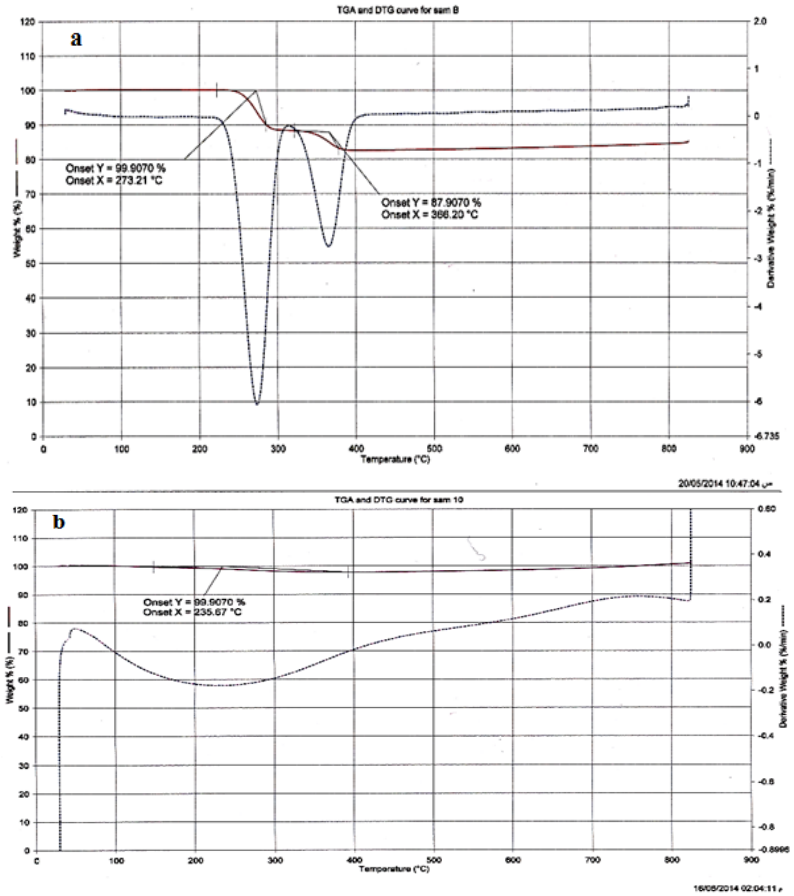

Figure12-TGA and DTG of a-as synthesized yttrium hydroxide by hydrothermal method and b-after being calcined at 1000°C

The suggested formula of the present hydroxide is $Y_2(OH)_{5.8}(NO_3)_{0.2}$ The calculated weight losses for this formula in the two steps of decomposition (12.4 and 6.83 respectively) were comparable with the observed values. At temperature above 400°C, no further weight loss took place which suggests the perfection of Y_2O_3 crystallization [9,26]. The TG curve of the as prepared hydroxide calcinated at 1000 °C (Figure -12 -b) showed no weight loss up to 230°C. Then a weight loss of 0.1% took place at peak temperature 255.29 °C as was indicated by the DTG curve attributed to absorbed moisture from the atmosphere. No further weight loss was observed above this temperature which refers to the stability and perfection of Y_2O_3 crystallinity [9,26]. The TG curve of microwave synthesized yttrium hydroxide shown in Figure (-13- a) exhibited four steps of thermal decomposition with a total weight loss of about 20.1. The first three steps involved weight losses of 1.12, 7.23 and 6.33 % at the temperature ranges: 30-145,145-315 and 385-412 °C at DTG peak temperatures: 102.9, 275.32, and 357.46 °C respectively.

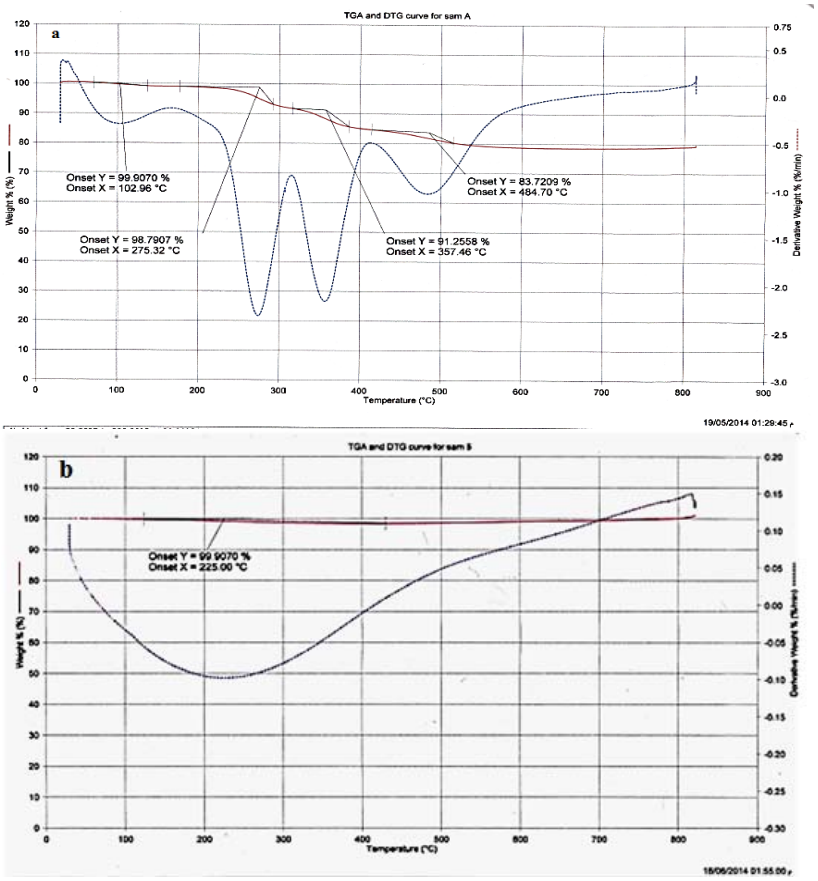

Figure 13-TGA and DTG of a-as synthsized yttrium hydroxide by microwave and b- after being calcined at 1000°C

The three steps were attributed to the gradual evaporation of about 0.18, 1.253 and 1.11 H_2O molecules for the gradual conversion of yttrium hydroxide precursor to the corresponding oxide[11]. The fourth step of thermal decomposition occurred at temperature range 412-515 ° C at DTG temperature 484.70 ° C with total weight loss 5.424 % and was attributed to the loss of the remaining water (~0.532H_2O, 1.99%) and thermal decomposition of existing nitrate (0.21NO_2, 3.03%) which leads to the final conversion of hydroxide precursor to stable form of yttrium oxide nanocrystals [9, 11, 18,26,37,44, 45]. The suggested formula for the present hydroxide is $Y_2(OH)_{5.79}(NO_3)_{0.21}$. The calculated weight losses in the four steps for this formula (1.02, 7.08, 6.22 and 5.08% respectively) are almost comparable with the observed values. These results agree with the TG/DTG explanations reported earlier [37,44, 45]. It can be concluded that conversion of microwave produced yttrium hydroxide precursor to Y_2O_3 occurs at higher temperatures compared to that obtained by hydrothermal method. The TG curve of Y_2O_3 obtained on heat treatment of microwave synthesized yttrium hydroxide at 1000°C for 3h (Figures-13-b) showed similar thermal behavior and stability to that of hydrothermal method, as no thermal decomposition was observed up to 210 °C. At temperature range 210-400°C a weight loss of 0.1% occurred at peak temperature 225°C as was indicated by the DTG curve which may be attributed to the evaporation of water embedded during crystallization of Y_2O_3 nanoparticles on calcination.

Conclusions

Yttrium oxide nanoparticles were synthesized successfully by calcination of yttrium hydroxide produced by hydrothermal and microwave hydrothermal methods at 500, 700, and 1000°C. The produced nanostructures were characterized by x-ray diffraction, FTIR , SEM and AFM. The SEM images showed variation of morphology with temperature. Calcination of yttrium hydroxide produced by hydrothermal and microwave hydrothermal methods at 1000°C gave nanorods and worm or neck-like nanostructures respectively. Thermo gravimetric analysis showed that calcination of as prepared

yttrium hydroxide by hydrothermal method was converted to yttrium oxide at lower temperature than that of microwave method.

Acknowledgment

The authors wish to thank Dr. Abdul-Kareem Mohamed Ali for his big cooperation and for performing the AFM analysis of the studied samples

References

1. Chen S., Lin J. and Wu J. **2014**. Facile synthesis of Y_2O_3:Dy^{3+} nanorods and its application in dye-sensitized solar cells *Applied Surface Science*, 293, pp. 202– 206.
2. Sohn S., Kwon, Y., Kim, Y. and Kim, D. **2004**. Synthesis and characterization of near-monodisperse yttria particles by homogeneous precipitation method. *Powder Technology*, 142 (2–3) pp: 136–153.
3. Alves, A., Bergmann, C. P. and Berutti, F. A. **2013**. *Novel Synthesis and Characterization of Nanostructured Materials*. Engineering Materials, Chapter 2: Combustion Synthesis. Springer-Verlag Berlin Heidelberg, pp: 11-22
4. Soga K ., Okumura Y., Tsuji K. and Venkatachalam, N. **2009**. Effect of K_3PO_4 addition as sintering inhibitor during calcination of Y_2O_3 nanoparticle. *Journal of Physics*: *Third International Symposium on Atomic Technology IOP* , 191, pp:1-7.
5. Munoz R. **2011**. Co-precipitation of Y_2O_3 powder, MSc. Thesis, Department of Materials Science and Engineering , MH265X, KTH ,Stockholm, Sweden
6. Ahlawat, R. and Aghamkar, P. **2014**. Influence of Annealing Temperature on Y_2O_3:SiO_2 Nanocomposite prepared by sol gel process. *Acta Physica Polonica* A, 126(3), pp: 736-739.
7. Yongqing, Z. , Zihua, Y., Shiwen D., Mande, Q., Jian, Z. **2003.** Synthesis and characterization of Y_2O_3: Eu nano powder via EDTA complexing sol–gel process. *Materials Letters,* 57, pp: 2901–2906
8. Vázquez, R. M., Hernández, M. G., Marure, A. L., Camacho, P. Y. L., Ramírez, Á. J. M. and Conde, H. I. B. **.2014**. Sol-gel Synthesis and Antioxidant Properties of Yttrium Oxide nanocrystallites incorporating P-123. *Materials,* 7, pp: 6768-6778
9. Aghazadeh, M., Ghaemi, M., Nozad, G. A., Yousefi, T. and Jangju, E. **2011**. Yttrium Oxide nanoparticles prepared by heat treatment of cathodically grown yttrium hydroxide. *International Scholarly Research Network, ISRN Ceramics*, 2011, pp: 1-6.
10. Andelman, T., Gordonov, S., Busto, G., Moghe, P. V, Riman, R. E. **2010**. Synthesis and Cytotoxicity of Y_2O_3 Nanoparticles of various morphologies. *Nanoscale Research Lett*ers, 5, pp: 263–273.
11. Li, N. and Yanagisawa, K. **2010.** *Yttrium Oxide Nanowires Nanowires Science and Technology*, book edited by: Nicoleta Lupu, INTECH, Croatia, Chapter 8, pp: 151-163.
12. Cristea, L. and Piticescu, R. **2002**. The kinetics study of the hydrothermal synthesis of the ZrO_2-Y_2O_3-Al_2O_3 system powders. *Metal,* 14 – 16(5), pp: 1-4 .
13. Zhong, S., Wang, S., Xu, H., Hou, H., Wen, Z., Li, P., Wang, S. and Xu, R. **2009**. Spindlelike Y_2O_3:Eu^{3+} nanorod bundles: Hydrothermal synthesis and photoluminescence properties. *Journal of Materials Science*, 44(14), pp: 3687-3693.
14. Larimi, Z. M., Amirabadizadeh A., and Zelati A. **2011**. Synthesis of Y_2O_3 nanoparticles by modified transient morphology method. *International Conference on Chemistry and Chemical Process IPCBEE*, IACSIT Press, Singapore, 10 (2011), pp: 86-90
15. Jayaramaiah, J.R., Lakshminarasappa, B.N. and Nagabhushana, B.M. **2011**.Synthesis, characterization and thermoluminescence studies of Y_2O_3:Sm^{3+} nanophosphor, *International Journal of Luminescence and Applications*, 1 (II), pp: 46-48
16. Mimani, T. and Patil K.C. **2001.** Solution combustion synthesis of nanoscale oxides and their composites. *Material Physics Mechanics*, 4, pp: 134-137.
17. Mouzon, J. and Oden, M.**. 2007.** Alternative method to precipitation techniques for synthesizing yttrium oxide nanopowder, *Powder Technology*, 177, pp: 77-82.
18. Ranjbar, M., Mannan, S., Yousefi, M. and Shalmashi, A. **2013.** Yttria nanoparticles prepared from salicylic acid-Y(III) nanocomposite as a new precursor. *American Chemical Science Journal* ,3(1): 1-10

19. Cheng, Xu. **.1999.** Synthesis of nanometer-sized yttrium oxide particles in diisooctyl sodium sulphosuccinate (AOT)/isooctane reverse micelle solution. *MSc Thesis*, Faculty of the Virginia Polytechnic Institute and State University, Blacksburg, Virginia.

20. Khollam, Y.B, Deshpande, A.S., Patil, A.J., Potdar, H.S. and Deshpande, S.B. **2001**. Synthesis of yttria stabilized cubic zirconia (YSZ) powders by microwave-hydrothermal route. *Materials Chemistry and Physics,* 71(3), pp: 235–241.

21. Panneerselvam, M., Subanna, G.N., and Rao, K. J. **2001.**Translucent yttrium aluminum garnet: Microwave-assisted route to synthesis and processing. *J. Mater. Res*., 16(10), pp: 2773-2776.

22. Mangalaraja R.V., Ramam, K.V.S., Ravi, J., Camurri, C. P. **2007** . Microwave-flash combustion synthesis of yttria nanopowders. *Materials Science-Poland*, 25(4), pp: 1075-1080.

23. Mann R., Laishram K. and Malhan N. **2011**. Synthesis of highly sinterable neodymium ion doped yttrium oxide nanopowders by microwave assisted nitrate-alanine gel combustion. *Transactions of the Indian Ceramic Society*, 70(2), pp: 87-91.

24. Potdevin, A., Pradal, N., François, M.-L., Chadeyron, G., Boyer, D. and Mahiou, R. **2012**. *Microwave-induced combustion synthesis of luminescent aluminate powders . Sintering - Methods and Products* Edited by Volodymyr Shatokha, , Publisher InTech, , , Published in print edition, Chapter 9, pp:189-212.

25. Mao Y., Huang, J. Y., Ostroumov, R. Wang, K. L. and Chang, J. P. **2008**. Synthesis and luminescence properties of erbium-doped Y_2O_3 Nanotubes *J. Physical. Chemistry. C*, 112*,* pp: 2278-2285.

26. Somiya, S. and Roy, R. **2000**. Hydrothermal synthesis of fine oxide powders. *Bullutin of. Material Science*, 23(6), pp: 453–460.

27. Bodapati S. **2011.** Mechanisms of yttrium oxide toxicity in HEK293 cells MSc Thesis, Marshall University, Department of Biology, Huntington , West Virginia.

28. Xu X. Sun, X., Liu, H. Li, J-G. Li, X. Huo, D. and Liu, S. **2012**. Synthesis of mono- dispersed spherical yttrium aluminum garnet (YAG) powders by a homogeneous precipitation method, *Journal of the American Ceramic Society*, 95 (12), pp: 3821-3826.

29. Wua X., Taoa Y., Gaoa F., Donga L., and Hua Z.. **2005.** Preparation and photoluminescence of yttrium hydroxide and yttrium oxide doped with europium nanowires. *Journal of Crystal Growth,* 277, pp: 643–649.

30. Sharma P., Jilavi M. H., NAû R., and Schmidt H. **1998**. Seeding effect in hydrothermal synthesis of nanosize yttria. *Journal of Materials Science Letters* , 17(10), pp: 823-825.

31. Pandey A., Dey R. and Rai V. K.**2013**. Sensitization effect of Yb^{3+} in upconversion luminescence of Eu^{3+} codoped Y_2O_3 phosphor. *Journal of Physical Chemistry and Biophysics*, 3(5), pp:1-3.

32. Nguyen T.-D., and Ono T. **.2009**. General two-phase routes to synthesize colloidal metal oxide nanocrystals: simple synthesis and their ordered self-assembly structures. *Journal of Physical Chemistry C* , 113(26), pp:1- 7.

33. Sung J.M., Lin S.E., and Wei W.C. J. **2007** .Synthesis and reaction kinetics for mono dispersive Y_2O_3:Tb^{3+} spherical phosphor particles. *Journal of the European Ceramic Society* , 27, pp: 2605–2611.

34. Gomes M. A. , Valerio M. E. G., and Macedo Z. S.. **2011.** Particle size control of Y_2O_3:Eu^{3+} prepared via a coconut water-assisted sol-gel method. *Journal of Nanomaterials*, 2011, pp:1- 6.

35. Brahme N., Gupta A., Bisen D.P. and Kurrey U. **2012.** Thermo luminescence study of Y_2O_3: Tb. *Recent Research in Science and Technology*, 4(8): 130-132.

36. Monshi A., Foroughi M. R., and Monshi M. R. **2012**. Modified, Scherrer Equation to Estimate More Accurately Nano-Crystallite Size Using XRD. *World Journal of Nano Science and Engineering,* 2, pp: 154-160.

37. Ermakov R. P., Voronov V.V., and Fedorov P. P. **2013**, X-Ray diffraction study of the phase and morphology changes in yttrium compound nanoparticles. *Nanosystems: Physics, Chemistry, Mathematics*, 4 (2), pp: 196–205.

38. Jeong, K..J. and Bae, D. S **. 2012.** Synthesis and Characterization of Y_2O_3 powders by a modified solvothermal process**.** *Korean Journal of Material Research*, 22(2), pp: 78-81

39. Christopher, A. Schwartz, T. and Schwartz, J. **2007** .Surface modification of Y_2O_3 nanoparticles, *Langmuir*, 23*,* pp: 9158-9161

40. Nguyen T-D., Dinh C-T. and Do T.-O. **2011**. A general procedure to synthesize highly crystalline metal oxide and mixed oxide nanocrystals in aqueous medium and photocatalytic activity of metal/oxide nanohybrids, *Nanoscale*, 3, pp:1861-1873.

41. Gougousi T. and Chen Z., **2008**. Deposition of yttrium oxide thin films in supercritical carbon dioxide. *Thin Solid Films*, 516, pp: 6197–6204.

42. Kokuoz B. Y., Serivalsatit K., Kokuoz B., Geiculescu O., McCormick E., and Ballatow J., **2009**. Er-Doped Y_2O_3 Nanoparticles: A Comparison of Different Synthesis Methods. *Journal of the American Ceramic Society,* 92 (10), pp: 2247–2253.

43. Lakshminarasappa B. N., Jayaramaiah J.R., and Nagabhushana B.M. **2012.** Thermoluminescence of combustion synthesized yttrium oxide**.** *Powder Technology,* 217*,* pp: 7–10.

44. Zhang N., Liu X., Yi R., Shi R., Gao G., and Qiu G. **2008**. Selective and controlled synthesis of single-crystalline yttrium hydroxide/oxide nanosheets and nanotubes. *Journal of Physical. Chemistry* C, 112, pp: 17788–17795.

45. Ahn J.-H. , Kim Y.-J., and Wang, G.**2010.** Hydrothermally Processed Oxide Nanostructures and Their Lithium–ion Storage Properties. *Nanoscale Research Letters*, 5, pp: 1841–1845.